Journal of Food Engineering 92 (2009) 172–181

Contents lists available at ScienceDirect

Journal of Food Engineering

journal homepage: www.elsevier.com/locate/jfoodeng

Tracer gas technique: A new approach for steady state infiltration rate measurement of open refrigerated display cases

Mazyar Amin [a,*], Dana Dabiri [a], Homayun K. Navaz [b]

[a] Aeronautics and Astronautics Department, University of Washington, Seattle, Washington 98195, USA
[b] Mechanical Engineering Department, Kettering University, 1700 University Ave., Flint, Michigan 48504, USA

ARTICLE INFO

Article history:
Received 30 May 2008
Received in revised form 21 October 2008
Accepted 25 October 2008
Available online 17 November 2008

Keywords:
Infiltration
Entrainment
Tracer gas
Air curtain
Open display case
Refrigeration
Measurement

ABSTRACT

A new approach, combining experimental and analytical methods, for finding the infiltration rate of outside warm air into open refrigerated display cases is introduced. This method is based on direct measurements and is more reliable and accurate than conventional techniques. Although a typical display case usually benefits from an air curtain at its opening to reduce the infiltration of the warm ambient air into the system, still the infiltration accounts for up to 75% of the total cooling load of their refrigeration system. In 1999, for example, about 69,000 of such display cases were operating in the supermarkets and grocery stores of the USA with annual energy consumption more than 1000 GW-hr (California Energy Commission (CEC) and Southern California Edison (SCE) Co., (2003). Private Communications.). Therefore, determining the exact amount of their infiltration rate and improving their performance are of great importance. In this method, a tracer gas is released into the air inside the duct of a display case and after mixing, the mixture discharges into the display area and ambient through the air curtain and/or the perforated back panel of the display case. This technique is based upon the concentration measurements of the tracer gas at three locations: *Discharge* duct, return duct and the ambient. Finding the percentage of the tracer gas that is lost (by escaping into the ambient) between the *Discharge* and the return ducts forms the fundamental of this approach. By analyzing the mass conservation around the air curtain of the display case, a relationship between the tracer gas concentration and the infiltration rate can be established.

1. Introduction

Open refrigerated display cases (*ORDC*s) are widely used in supermarkets in the United States and around the world to display and store food and dairy products in a prescribed allowable temperature. Supermarkets are one of the most energy intensive commercial building types in the United States, with annual energy use of 45–65 kW-h/ft^2 69000 stores (CEC-SCE, 2003). A 15% improvement in the performance of the systems can yield more than $100 million only in the United States. Most of such systems have to operate 24 h a day, seven days a week. Vertical and horizontal *ORDC*s are both popular in supermarkets and since they lack doors, there are no physical barriers that can prevent the penetration of the exterior warmer air into the cold interior (in some supermarkets however, the opening of vertical *ORDC*s may be covered by PVC strips at night, which are then removed during the day). As a consequence, the cooling loads of *ORDC*s are higher than similar designs that have from doors. It should be mentioned that for certain applications, ORDC are preferred to the display cases with doors; in fact in *ORDC*s the access to the products increases and the fogging problem on the inner side of the doors will not exist anymore.

According to Howell and Adams (1991), up to 75% of the total cooling load of a vertical *ORDC* is due to the infiltration of outside air through the air curtain. Obviously, the higher cooling load will bring about longer operation of the refrigeration system that in turn increases the energy consumption. Consequently, the need to improve the design of the *ORDC*s has been felt from decades ago and much effort has gone into developing more cost effective and energy efficient systems. Air curtain research has ranged from analytical studies (Hayes and Stoecker, 1969) to experimental (Field et al., 2002; Navaz et al., 2002, 2005; Rouaud and Havet, 2006; Amin et al., 2008) and computational (Stribling et al., 1997; Cortella et al., 2001; Axell and Fahlen, 2002; Navaz et al., 2005; Foster et al., 2005; Rouaud and Havet, 2006) investigations. One of the conventional methods for the infiltration measurement is based on collection of condensate dripping off the evaporator of the refrigeration system (Faramarzi et al., 2004). The amount of this condensate is proportional to the humidity ratio in the ambient that is determined from the dry bulb and wet bulb temperature and humidity measurements. Then the mass of the infiltrated air

* Corresponding author. Tel.: +1 206 931 7621; fax: +1 206 543 0217.
E-mail addresses: mazamin@yahoo.com, mazyar@u.washington.edu (M. Amin).

0260-8774/$ - see front matter © 2008 Elsevier Ltd. All rights reserved.
doi:10.1016/j.jfoodeng.2008.10.039

Nomenclature

Am	ambient
BP	back panel
C	mass concentration of tracer gas
CFD	computation fluid dynamics
DAG	discharge air grille
Dis	discharge
Inf	infiltration
Inj	injection
$\dot{m}$	mass flow rate
NIR	non-dimensional infiltration rate
ORDC	open refrigerated display case
ppm	particles per million particles
Q	volumetric flow rate
RAG	return air grille
S	surface area
Spl	spillage or spilled flow
t	time
TLV	threshold limit value
X	volumetric concentration
ρ	density
η	thermal entrainment

can be calculated from the humidity ratio and with the knowledge of the time duration of the condensate collection. The method is very time-consuming and somewhat indirect. Another method proposed by Rigot (1990), and Navaz et al. (2005) establishes a correlation among the infiltrated warm air and enthalpies of the air at the discharge air grille (*DAG*), return air grille (*RAG*) and the ambient environment outside the *ORDC*. These enthalpies can easily be calculated by temperature measurements. This technique, too, is time-consuming since the average temperature measurements require the velocity profiles at the *DAG* and *RAG*. These techniques are not only tedious and time-consuming, but they also rely on the measurements of other flow parameters to find the amount of infiltrated warm air into the display cases. In this work, we will show that the amount of infiltrated warm air can be related to the mass fraction of a tracer gas measured at the *DAG*, *RAG* and ambient. These mass fractions are directly related to the infiltration rate. Generally, this method is a new approach by which the infiltration rate can be measured faster and more accurately and is particularly more beneficial when several infiltration tests are required to be performed in a short time.

2. Description of *ORDC* and flow pattern

In HVAC applications, tracer gas has been used to determine the duration that the air inside a confined space can be completely changed and refreshed (ASHRAE, 2005), or to identify the spaces in a building that the air is stagnant. Although this work specifically concentrates on a vertical *ORDC*, the intention of this study is to introduce and establish a procedure and a guideline for infiltration measurement of all types of *ORDC*s that circulate air. The display case under study benefits from an air curtain and back panel (*BP*) flow. The air curtain is mostly responsible to prevent the penetration of outside into the display case; while *BP* flow is in charge of the maintaining the temperature of the products at desired level. Fig. 1 depicts the side view of an *ORDC* with the schematic of the flow patterns around it. Moving in the downstream direction of the air curtain, the outside air can be entrained throughout the entire height of the display case opening and the air curtain. A portion of the mixture of the airs is drawn into the *RAG* and the rest spills into the room.

In this study, the fundamental of tracer gas technique is based on the loss of the tracer gas from the *Discharge* to the *RAG*. Here, the *Discharge* accounts for all the locations on the display case surfaces where the flow leaves the interior ducts, i.e. at the *DAG* and *BP*. The air temperature and tracer gas concentration at the two latter locations are almost identical. However, the concentration in the *RAG* is smaller than that at the *Discharge* due to entrainment of flow from the ambient into the air curtain and subsequently infiltration of the entrained air into the *RAG*. The total mass flow rate at the *RAG* is equal to that of the *Discharge* as:

$$\dot{m}_{RAG} = \dot{m}_{Discharge} = \dot{m}_{DAG} + \dot{m}_{BP} \quad (1)$$

After the tracer gas is released into the *primary flow* (*primary flow* is the flow in the upstream of the tracer gas injection location), a portion of the gas eventually abandons the system and disperses into the ambient. The difference between the concentrations at the *RAG* and *Discharge* will dictate the amount of this infiltration. In an ideal case where no infiltration occurs, the concentrations at the *RAG* and the *Discharge* will be the same. In contrast, in the worst but perhaps an unrealistic scenario, all the tracer gas at the *Discharge* escapes into the ambient very quickly, and the *RAG* will have very low to zero concentration. In limit, zero *RAG* concentration accounts for the maximum possible infiltration of ambient air into the display case.

It should be mentioned that an analogy can be made between the tracer gas with higher concentration and the air with lower temperature: both high-concentrate tracer gas and cold air at the *Discharge* are partially disperse and lost in the ambient and instead low-concentrate tracer gas or warm air are replaced.

3. Relation between infiltration rate and tracer gas concentration

To quantify the description of the infiltration given above, a mathematical analysis of the flow through and about the *ODRC* is performed. Revisiting Fig. 1, a rectangular control volume (*CV*) can be drawn around the air curtain region. The *CV* spans vertically from the *DAG* to the *RAG*, and horizontally from the front edges of the shelves to the outermost of the *RAG*. Ambient air entrainment into the *CV* as well as flow spillage near the *RAG* can also occur. The flow through the *CV* can be summarized as: two inlets that include the *Discharge* (*DAG* + *BP*) flow and entrained flow from the ambient, and two outlets that include the *RAG* flow and the spilled flow. In addition, the concentration of the tracer gas in the entrained flow is directly dependent on the concentration of the ambient. It should be noted, however, the concentrations at the ambient, *RAG* and *Discharge* are tailored to each other such that change of one will directly influence the others too. Fig. 2 presents a more detailed view of the flow in order to better understand and analyze the flow through and within the *CV*. The concentration at the *DAG* is almost identical to that of the *ORDC* cavity, since the flow characteristics within the cavity, which is between the *BP* and the *CV*, are mostly associated with the *BP* flow properties. As a result, for convenience in the analysis, one may combine the *DAG* and the *BP* and introduce only one *Discharge* mass flow rate ($\dot{m}_{Dis}$) and mass concentration (C_{Dis}) as shown in Fig. 2 to represent both boundaries. It should be emphasized that there is a subtle difference between infiltration and entrainment. In the past, misinterpretations have sometime lead to equating these two terms. Infiltration is defined as the amount of outside air that can ingress

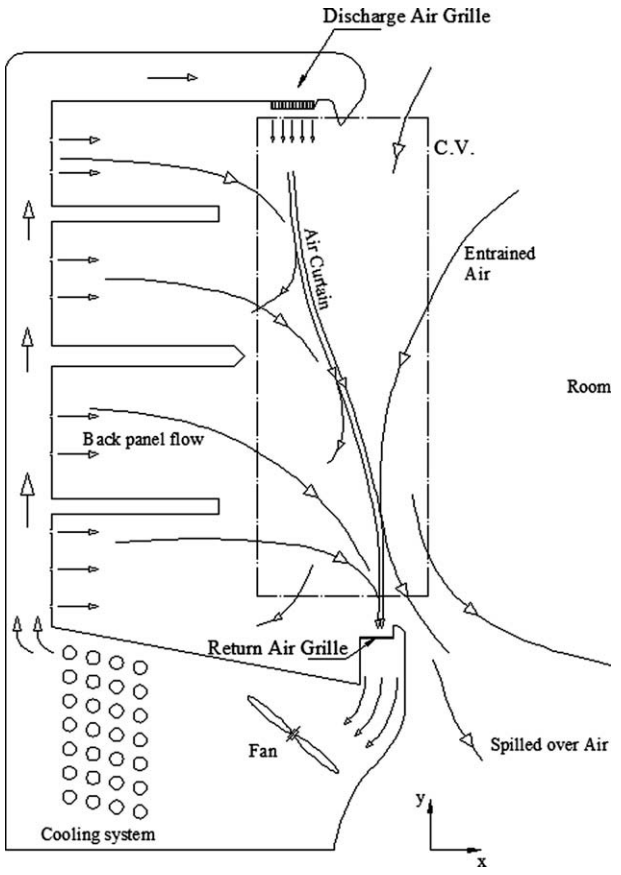

Fig. 1. Schematic of the side view of a typical *ORDC*.

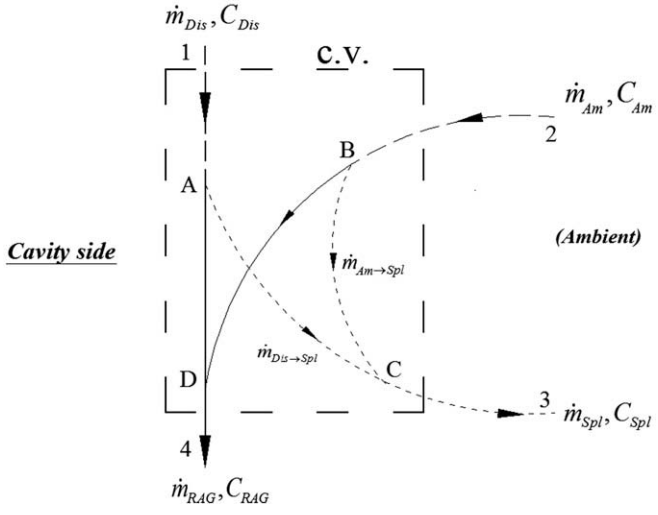

Fig. 2. Simulation of the flow patterns at the control volume.

the *RAG*; in fact, not all the entrained air is drawn into the *RAG* but just a portion of it is drawn in, which is defined as the infiltrated flow. The rest of the entrained flow moves to the ambient after some mixing with the flow inside the *CV*.

It should be noted here that in this analysis, the flow interaction between the control volume and the flow within the cavity is ignored. This is because it is assumed (Navaz et al., 2002) that with the presence of the air curtain and the steady performance of the refrigeration system, the temperatures of the products, cavity, and *Discharge* will be almost the same and ideally no flow passes across the air curtain to the other side. By using this result and knowing that temperature and tracer gas concentration are counterparts (the higher concentration of the tracer gas in the flow accounts for lower temperature), one can conclude that the concentrations of the tracer gas over the products and within the cavity are the same as that of the *Discharge*. Therefore, even if we add two more lines (one from the cavity to the *CV* and the other from the *CV* to the cavity) they will have identical flow rates and concentrations. As a result, no change will be imposed from the cavity side into the *CV*.

As also shown in this figure, the flow between points 2 and B accounts for the entrained air; the portion of the entrained air which splits at point B and enters the *RAG* at point D corresponds to the infiltration, while the remaining portion contributes to the spilled air (line B → C). The solid lines denote the flow that will eventually enter the *RAG* while the short dashed lines symbolize the flow that will enter the ambient. Results of Navaz et al. (2002) and CFD results of Amin et al. (2008), performed by Fluent commercial code, indicated that almost all the flow that leaves the *CV* and entering the ambient, exits from the lower part of the vertical boundary close to the *RAG*, while almost all the entrainment occurs from the rest of the outerside vertical boundary (Fig. 3a). From the contours of Fig. 3b, it is clear that the tracer gas (CO_2 here) is accumulated near the floor and the concentration near the air curtain is noticeably lower at any height across the air curtain. Therefore, the concept of showing the entrained and exiting flows each by one line is valid as long as we deal with the total (integral) of the entrained mass flow rates or exiting mass flow rates. As to the concentrations, the average values should be considered along the *CV* surfaces.

As further shown in Fig. 2, the *Discharge* flow enters the *CV* through line 1 → A (the downward vertical direction of the line should not imply only the *DAG* flow, but it represents both the *DAG* and *BP* flows). Also, as stated before, a portion of the entrained flow (line 2 → B) is infiltrated into the *RAG* (through line B → D). The other portion of the *Discharge* flow that does not leave the *CV* and still is highly concentrated with the tracer gas, heads towards the *RAG* (line A → D) and before entering the *RAG* (point D) starts mixing with the flow that is infiltrated (line B → D). Line D → 4 carries the mixed flow to the *RAG* to be blown over the cooling coils by the fan. The mixing points C and D represent all the physical points inside the *CV* where mixings occurs.

Now that the *CV* and flow through it are properly defined, the conservation of the total flow rate inside the *ORDC* duct from the *RAG* to the *Discharge* can be expressed. The tracer gas is injected within this duct between the *RAG* and *Discharge*. The total flow rate is defined as the flow rate of the "air + tracer gas" mixture and its conservation inside the duct can be written as:

$$\dot{m}_{Dis} - \dot{m}_{RAG} = \dot{m}_{Inj} \tag{2}$$

It is emphasized again that infiltration is defined as a portion of the ambient flow that will enter the *RAG*. The ambient air may contain some tracer gas too, thus its concentration should not be considered to be zero. The flow rate through line A → D is $(\dot{m}_{Dis} - \dot{m}_{Dis\to Spl})$ and at point D, the conservation of the tracer gas mass can be expressed as:

$$\dot{m}_{RAG}C_{RAG} = \dot{m}_{Inf}C_{Inf} + (\dot{m}_{Dis} - \dot{m}_{Dis\to Spl})C_{Dis} \tag{3a}$$

where C is the mass concentration of the tracer gas and is defined as:

$$C = \frac{\dot{m}_{CO_2}}{\dot{m}_{CO_2} + \dot{m}_{air}} \tag{3b}$$

In addition, conservation of total mass at point D will be:

$$\dot{m}_{RAG} = \dot{m}_{Inf} + (\dot{m}_{Dis} - \dot{m}_{Dis\to Spl}),$$
$$\Rightarrow \dot{m}_{Dis} - \dot{m}_{RAG} = \dot{m}_{Dis\to Spl} - \dot{m}_{Inf} \tag{4}$$

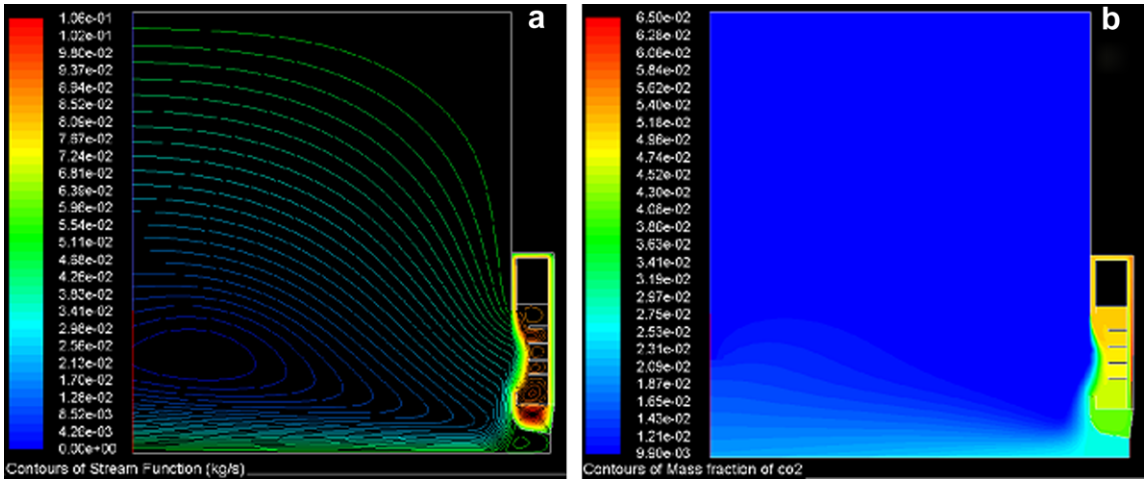

Fig. 3. CFD simulation by Amin et al. (2008). (a) Streamlines and (b) tracer gas concentration.

By combining Eqs. (2) and (4) one gets:

$$\dot{m}_{Dis\to Spl} - \dot{m}_{Inf} = \dot{m}_{Inj},$$
$$\Rightarrow \dot{m}_{Dis\to Spl} = \dot{m}_{Inf} + \dot{m}_{Inj} \tag{5}$$

Mass conservation of tracer gas at point D results in:

$$\dot{m}_{RAG}C_{RAG} = \dot{m}_{Inf}C_{Inf} + (\dot{m}_{RAG} - \dot{m}_{Inf})C_{Dis} \tag{6}$$

And by solving for $\dot{m}_{Inf}$ we'll get:

$$\dot{m}_{Inf} = \dot{m}_{RAG}\frac{C_{Dis} - C_{RAG}}{C_{Dis} - C_{Inf}} \tag{7}$$

In Fig. 2, since the ambient air, is first entrained into the *CV* and then infiltrated into the *RAG*, one may conclude that $C_{Inf} = C_{Am}$. Therefore, Eq. (8) can be rewritten as:

$$\dot{m}_{Inf} = \dot{m}_{RAG}\frac{C_{Dis} - C_{RAG}}{C_{Dis} - C_{Am}} \tag{8}$$

This equation presents the amount of the infiltrated flow from the ambient, which can be calculated by knowing the concentrations at the *RAG*, *Discharge*, and ambient, as well as the total flow rate at the *RAG*. This equation is valid as long as the concentration at the ambient is different from that of the *Discharge*. Faramarzi et al. (2008), have shown that the mass flow rate at the *RAG* ($\dot{m}_{RAG}$), can be readily found by knowing the concentrations of tracer gas at the *RAG* and *DAG* and also the mass flow rate of the injected tracer gas. The advantage of this method is that the flow rate measurement can be performed when the infiltration rate measurement is in the process. More importantly, this technique does not require the knowledge about the velocity profile for the flow measurement.

$$\dot{m}_{\text{air}} = \frac{\dot{m}_{inj}}{\left[\frac{C_{Dis}}{1-C_{Dis}} - \frac{C_{RAG}}{1-C_{RAG}}\right]} \tag{9}$$

During our experiments, it was quite evident that in a large test laboratory with proper ventilation, the ambient space behaved as a sink for the tracer gas. Such a condition may cause a very small or even negligible tracer gas concentration in the ambient. In contrast, in a small laboratory, the concentrations of the ambient room will noticeably rise such that it may be comparable to those of the *Discharge* or the *RAG*. In such a situation, averaging the concentration in the vertical direction and along the outermost surface of the *CV* is necessary (averaging in z-direction and parallel to the *DAG* length can be helpful unless the *DAG* is long enough to simulate a quasi-2D air curtain). It is possible that even in a small room with an operating ventilation system, when the ambient (room) concentration significantly increases, it will eventually reach a steady condition. Another issue in the tracer gas technique is the presence of the tracer gas in nature or the ambient. This should not be of any concern in using Eq. (8) since the constant amount in nature is measured in all the measurement locations and will show up in all the concentration terms and will be canceled out when subtractions are performed in the numerator or denominator.

Due to the type and amount of the tracer gas that is used, the mass flow rate of the *RAG* can differ from the mass flow rate of the *primary flow*. In such a case, the $\dot{m}_{RAG}$ can be calculated as:

$$\dot{m}_{RAG} = \rho_{RAG}Q_{RAG} \tag{10}$$

and

$$Q_{RAG} = S_{RAG}V_{RAG} \tag{11}$$

where ρ, Q, S and V denote density, volumetric flow rate, *RAG* area, and average velocity normal to the *RAG* exit, respectively. On the other hand, the density at the *RAG* can be calculated from

$$\rho_{RAG} = C_{RAG}\,\rho_{\text{tracer\_gas}} + (1 - C_{RAG})\rho_{\text{air}} \tag{12}$$
$$\Rightarrow \dot{m}_{RAG} = \lfloor C_{RAG}\,\rho_{\text{tracer\_gas}} + (1 - C_{RAG})\rho_{\text{air}}\rfloor S_{RAG}V_{RAG} \tag{13}$$

The non-dimensional form of the infiltration rate (*NIR*) can now be defined by dividing both sides of Eq. (8) by $\dot{m}_{RAG}$

$$NIR = \frac{\dot{m}_{Inf}}{\dot{m}_{RAG}} = \frac{C_{Dis} - C_{RAG}}{C_{Dis} - C_{Am}} \tag{14}$$

NIR can be interpreted as the efficiency of an *ORDC* in infiltrating the outside air. The higher values of *NIR* represent higher infiltrations that are undesirable). For example, an *ORDC* that operates at a high speed and flow rate, can potentially infiltrate larger amount of outside warmer air ($\dot{m}_{Inf}$) compared to one which operates at a lower flow rate. However, it is likely that the former infiltrates less outside air mass flow rate per unit of the flow rate at the *RAG* $\left(\frac{\dot{m}_{Inf}}{\dot{m}_{RAG}}\right)$ than a lower speed display case. In such a case the higher-flow rate display case can be recognized as the more efficient display case with regards to the air curtain performance.

Eq. (14) resembles the *thermal entrainment* (η) used in some studies (Rigot, 1990; Field and Loth, 2006) given as:

$$\eta = \left|\frac{T_{DAG} - T_{RAG}}{T_{DAG} - T_{Am}}\right| \tag{15}$$

In limit, when the entire discharged tracer gas is drawn back into the return duct ($C_{RAG} = C_{DAG}$ in Eq. (14)) the infiltration goes to zero, which is consistent with $T_{DAG} = T_{RAG}$ and $\eta \to 0$ in

Eq. (15). Similarly, if no portion of the air from the *DAG* reaches the *RAG* (for instance when the air curtain breaks due to bending outward), the *RAG* concentration and temperature become identical to those of the room. Therefore, if $C_{Am} = C_{RAG}$ or similarly $T_{Am} = T_{RAG}$, they will yield equivalent results, i.e. $NIR \to 1$ and $\eta \to 1$, which represent the worst case scenario. Therefore, one may state this analogy as:

$$\frac{C_{Dis} - C_{RAG}}{C_{Dis} - C_{Am}} = \frac{T_{Dis} - T_{RAG}}{T_{Dis} - T_{Am}} \tag{16}$$

The percentage of the divergence of the flow rate (with tracer gas) at the *RAG* from the flow rate with no added tracer gas can be simply found (not described here) using Eq. (1):

$$\frac{\dot{m}_{RAG}}{\dot{m}_{air}} = \frac{(\dot{m}_{air} + \dot{m}_{CO_2})_{RAG}}{\dot{m}_{air}} = 1 + \left(\frac{\dot{m}_{CO_2}}{\dot{m}_{air}}\right)_{RAG} \tag{17a}$$

And by using Eq. (3b) one can find

$$\frac{\dot{m}_{CO_2}}{\dot{m}_{air}} = \frac{C}{1 - C} \tag{17b}$$

By combining Eqs. (17a and b) the divergence can be found as:

$$\frac{\dot{m}_{RAG}}{\dot{m}_{air}} - 1 = \frac{C_{RAG}}{1 - C_{RAG}} \tag{17c}$$

Also, normally the output of our gas analyzers is reported in term of volumetric concentrations, a conversion to mass concentration is required to suit Eqs. (8) and (14). By combining Eq. (3b) with its counterpart for volumetric concentration (Eq. (18)) one can get the conversion given by Eq. (19):

$$X = \frac{\dot{V}_{CO_2}}{\dot{V}_{CO_2} + \dot{V}_{air}} \tag{18}$$

$$C = \frac{R}{R + \frac{1}{X} - 1} \tag{19}$$

where $R = \frac{\rho_{tracer\_gas}}{\rho_{air}}$ and X is the volumetric concentration. Eqs. (17c) and (19) show that the divergence from actual flow rate depends on both the concentration of the gas, as well as the density of the tracer gas.

4. Experimental facility

In the following sub-sections, the components of the systems, procedure of the testing and the considerations that should be taken into account before and during the infiltration tests will be discussed.

4.1. Tracer gas selection

For proper conduction of the infiltration tests (will be explained later), a suitable tracer gas must be selected (ASTM, 2004). The main characteristic of a tracer gas should be its capability of perfectly following the *primary flow*, which requires their densities not to be too different. If this is not true, the high concentration of the tracer gas may significantly affect and change the density of the mixture (see also Eq. (17c), and Table 1). Flammability, health concerns, odor and taste physical and chemical damages to the environment, and tracer gas cost are some other factors in selecting a tracer gas.

With regards to the above factors, CO_2 gas was chosen for the current tests. CO_2 is also sometimes used for HVAC tests to quantify the number of air changes of a space per hour (ACH). It is naturally present in air and its concentration in the ambient usually varies between 300 and 500 ppm (particles per one million total particles). Concerning health issues, it is recommended that the concentration of CO_2 be less than 5000 ppm (ACGIH, 1971, and IDLH, 2007). In this work, dry-bone type CO_2 with 99.99% purity is used. Although, the purity of the injected gas does not affect the results of the experiment (since we are interested in the change of CO_2 concentration) it may affect the process of the test such as freezing during the expansion.

Table 1
Error in the mass flow rate at the *RAG* by adding tracer gas.

RAG concentration (%)		Divergence from the actual *RAG* mass flow rate (%)
Volumetric	Mass	
0.40	0.60	0.61
1.20	1.81	1.84
2.00	3.00	3.10

4.2. Injection system description

To achieve a uniform concentration of the tracer gas at the sampling locations, the gas was uniformly and continuously released into the air flow in along the length of the duct. For this purpose, a straight tube with several holes on its length was inserted within the duct of the display case. As in Fig. 4, the injection tube was inserted between the *RAG* and the *DAG*. The injection location was sufficiently far from the *Discharge* to allow the tracer gas to thoroughly mix with air before being sampled. Bearing the maximum health *TLV* in mind ($\sim$5000 ppm $\equiv$ 0.5% for CO_2), it was observed in our experiments that if the concentration within the in the *DAG* is about 25,000 ppm (2.5%), it will yield an ambient concentration around or below 5000 ppm. Four tanks through a manifold supplied the required CO_2 flow rate to provide 25,000 ppm at the discharges. A pressure regulator lowered the pressure down to 10 atm. Right before the injection tube, a flow control valve and an Alicat Scientific digital flowmeter were installed to adjust the injection rates manually and to measure it, respectively. The injection tube had 20 holes on it. The duration of injection was controlled by an adjustable timer which was coupled with a solenoid valve.

4.3. Sampling probes and tubes

According to Eq. (8), the samples should be taken at or very near the *RAG*, *DAG* and ambient. For getting more accurate results during the tests, the following locations were selected as shown in Fig. 4:

- About 0.8–1.2 m across the air curtain.
- Between the RAG and the injection point.
- Between the injection point and the Discharge (particularly before the DAG here).

The ducts sampling probes were inserted perpendicular to the flow at the locations where the flow was anticipated to be uniform and along the width of the duct. Since the gas analyzer used for this study had three channels and there were three sampling zones, one sample line was connected to each channel. Each sampling line that enters into the gas analyzer was already split into several branches across the length of the sampling section (Fig. 5), in order to allow for more uniform acquisition of data. Also three sampling probes were located at different heights near the *CV* (about 0.8–1.2 m across the *CV*, see Fig. 4) to monitor the variation of tracer gas concentration in the ambient. In our studies the aspect ration of the DAG was large (about 28) and the effect of 3-dimensionality in the flow field and concentration gradient along the length of the display case were relatively small and therefore only used three sampling probes were inserted along the length of *DAG* and *RAG*. Obviously, should the effect of 3-dimensionality is noticeable for instance due to small aspect ratios or inability to provide uniform flow across the length of the display case, one my consider inserting additional probes; however in such a case it is possible that

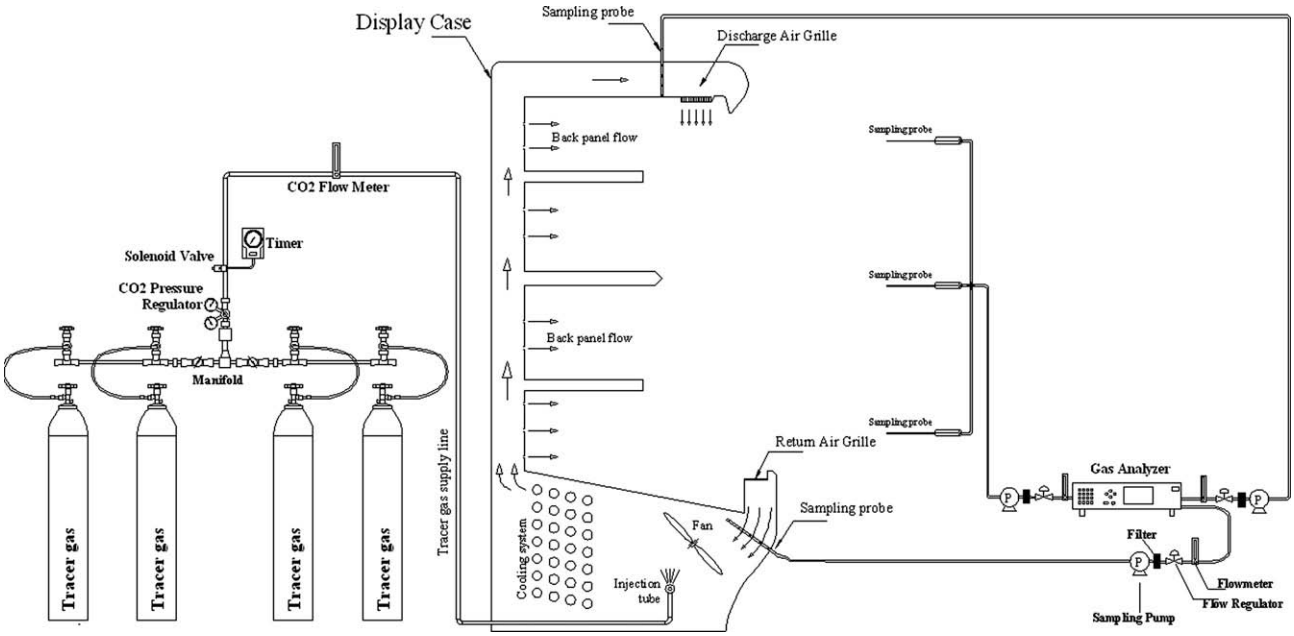

Fig. 4. Side view of a display case with injection and sampling systems set up.

more agitation more pronounced flow pattern changes, due to insertion of more probes, is traded for better sampling results.

4.4. Suction pumps, flow control valves and flow meters

Suction pumps draw the mixture of tracer gas and air from the desired points and transfer it to the gas analyzer. The pumps should be installed between the sampling probes and the gas analyzer and each gas analyzer channel requires one separate pump. A diaphragm pump was used for each channel and a flow meter with an adjustable pin valve was required to monitor and control the flow rate of the sampled flow. The sampling flow rate of each channel was about 0.5 liter/min.

4.5. Tracer gas analyzer

A Horiba gas analyzer (VA-3000) that utilizes non-dispersive infrared (NDIR) technology was used for measuring the concentration of the CO_2 tracer gas. This instrument includes three input channels as there are three sample inlets to the analyzer. The rate at which the samples were analyzed and concentrations were reported was 1 data/sec. By using Horiba's DL-3000 software, the data was logged and stored in a computer.

The repeatability, linearity and zero/span shift errors of the gas analyzer are, 0.5%, 1%, and 0.5% of the full scale value, respectively; while the sensitivity of the instrument was less than 1%. The resolution of the instrument is 1 ppm. The overall uncertainty is about ±480 ppm equivalent to ±1.9% of the full scale value.

5. Measurement procedures

5.1. Calibration of gas analyzer

For calibrating the gas analyzer, first, the system was "zeroed" by a gas with tracer gas concentration equal to zero. Next, a span gas with a known concentration of the tracer gas was flown into

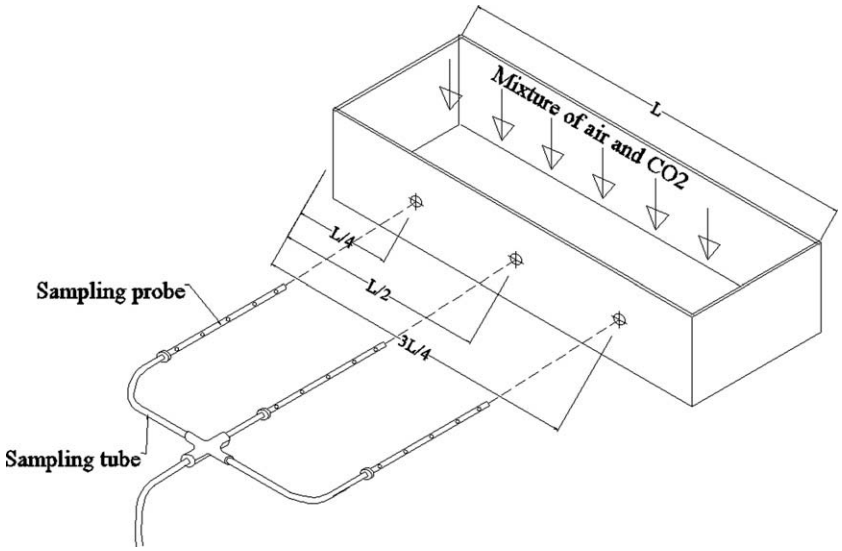

Fig. 5. Branching the sampling probes in a section of the display case duct.

the gas analyzer. By performing these two steps the analyzer will recognize its linear calibration through these two concentrations. In these experiments nitrogen was the zero gas and the span gas contained 24,350 ppm CO_2 (equivalent to 2.435% concentration). The flow rate of the calibration gasses was 0.5 liter/min

5.2. Procedures of infiltration rate measurement at steady state

After setting up the equipment as shown in Fig. 4 and when the gas analyzer is calibrated, the fans of the display case should run until the flow within the laboratory has reached steady state. The gas analyzer's suction pumps should also operate simultaneously to purge its channels from previous sampled gases. Next, the tracer gas is released into the air inside the duct, after which its concentration rises throughout the test facility. Depending upon several factors such as the size of the laboratory, the tracer gas injection flow rate, total flow rate of the display case, ventilation of the laboratory, dimension of the display case, and food level on the shelves, concentrations of different zones may take up to a few minutes for them to reach steady state. Due to this time delay, the release of the tracer gas should be continuous. In our test facility, the concentrations of the tracer gas reached almost constant values in all the sampling zones after a few minutes, and remained almost constant for long periods of time. This was due to two reasons. First, the large size of the laboratory acted as a sink for the tracer gas, and second, the ventilation of the laboratory played a significant role in removing ambient tracer gas from the laboratory. It should be noted that during the tests, the ventilation, ideally speaking, should not cause any draft or unwanted flow; otherwise it could affect the pattern and efficiency of the air curtain of the display case. In reality however, the flow inside and around a display case may be affected by the ventilation of the supermarket, air motion near the display case caused by the passing by customers, draft from supermarket's entrance, etc. Considering such effects requires a study for unsteady conditions, which is beyond the scopes of this study.

It should be added that the concentrations of the gas at the *DAG* and at the back panel are ideally the same and the derivation of Eq. (7) was with this assumption. It was verified in several cases that there were very minor differences between the *DAG* and *BP* concentrations.

6. Results

Fig. 6 presents the volumetric concentrations of CO_2 at the *DAG*, *RAG* and the ambient, as well as *NIR* obtained from Eq. (14). This figure shows the infiltration results starting with the release of the tracer gas until the injection was stopped, and after which the concentrations gradually declined to zero. The figure is trying to just introduce the test and portrait the variation of the concentrations in time during the entire length of a test from almost the start of injection until the concentrations go to zero. We purposefully undertake the test to large concentration gradients, which shows mild variations in room concentrations with respect to the variations of the *DAG* and *RAG* concentrations. It was not however, the intention of the authors to draw some quantitative conclusions out of that.

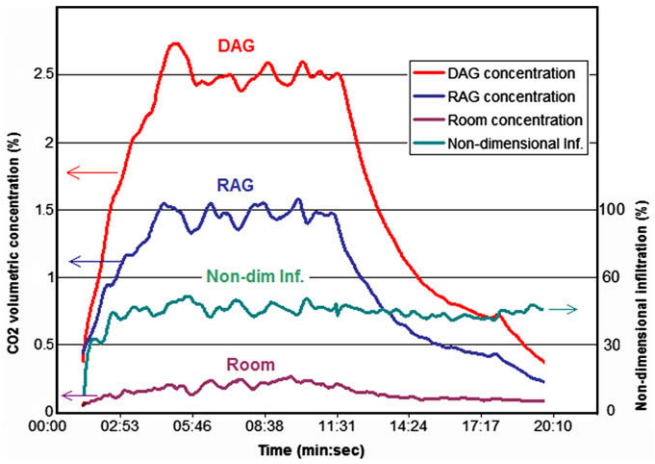

Fig. 6. Sample of tracer gas concentrations and non-dimensional infiltration of an *ORDC*.

After injecting the tracer gas, concentrations in all three regions (*DAG*, *RAG* and Ambient) start to grow until $t \approx 05{:}00$. During this period the rate of increase of concentration at the *DAG* was faster than the other regions. In most of our tests, the *DAG* concentration was maintained between 2.3% and 2.5%. From $t \approx 06{:}00$ to 12:00 the concentrations fluctuated around a mean value, which perhaps is due to small unsteadiness that may exist in the injection and samplings. Since concentration was almost steady during this period, it is desirable to dedicate most of the test duration and calculation of the *NIR* to this section. At $t \approx 12{:}00$, the release of the tracer gas was stopped; however, further data acquisition shows that *NIR* is still constant, taking the same values as before (up to $t \approx 20{:}00$). The value and trend of *NIR* variation is mostly dependent on the trend and gradient of the concentrations. For instance, before $t \approx 03{:}00$ the gradient of *DAG* concentration is greater than those of the *RAG* and ambient, and therefore the *NIR* is different from the middle section of the test ($03{:}00 < t < 12{:}00$). After $t \approx 12{:}00$, the *DAG* and *RAG* concentrations descended smoothly in the same manner; as a result the *NIR* takes almost the same value as that of the middle section of the test. Fig. 7a demonstrates the change of concentration with time during another test. The flow rate of the CO_2 injection was deliberately varied in time to examine the effect of concentration values on the *NIR*. At $t \approx 01{:}30$ the concentrations spike (encircled region) causes a spike in the *NIR* as well (Fig. 7b). After the spike, the tracer gas concentrations experience some periodic alternations, but the *NIR* remains almost unchanged. Hence, one may conclude that the amount of the tracer gas injection flow rate almost does not impact the *NIR* but it is the gradient of the change of concentrations which are of the greater importance. This however, does not mean that there are no restrictions for the amount of tracer gas release as it may significantly affect the average density in addition to the health effects. In the infiltration tests the duration of the tests is mostly contingent upon the flow speed and geometrical configuration of the display case. At slower speeds or lower flow rates, the measurements need to be performed for a longer period of time, since longer time is needed for the flow to circulate through the test case. Also at a constant fan speed, if the *DAG* and *RAG* become more distant, the travel distance and time both increase.

In such cases, since the simultaneous readings of the concentrations at the *DAG* and *RAG* do not belong to the same fluid regions, there will always be some time lag between the *RAG* and *DAG* concentrations, which explains the variations in the fluctuations seen in the *DAG* and *RAG* concentrations. Sometimes this time lag is positive and some times negative depending on the conditions at the sampling locations. For examining such delays, a portion of the concentration plots in Fig. 8a (inside the box) is shown in Fig. 8b. Points a and a′ are counterparts of local maxima on the *DAG* and *RAG* concentrations, respectively. The effect of increase in the *DAG* concentration at point a, appears as an increase in the *RAG* concentration, at point a′, after a delay of Δt_a.

A similar situation is seen for local minima at points b and b′ with a delay of Δt_b. The *NIR* at time t_a was seen (not shown here) to be larger than that of the situation at which both maxima took

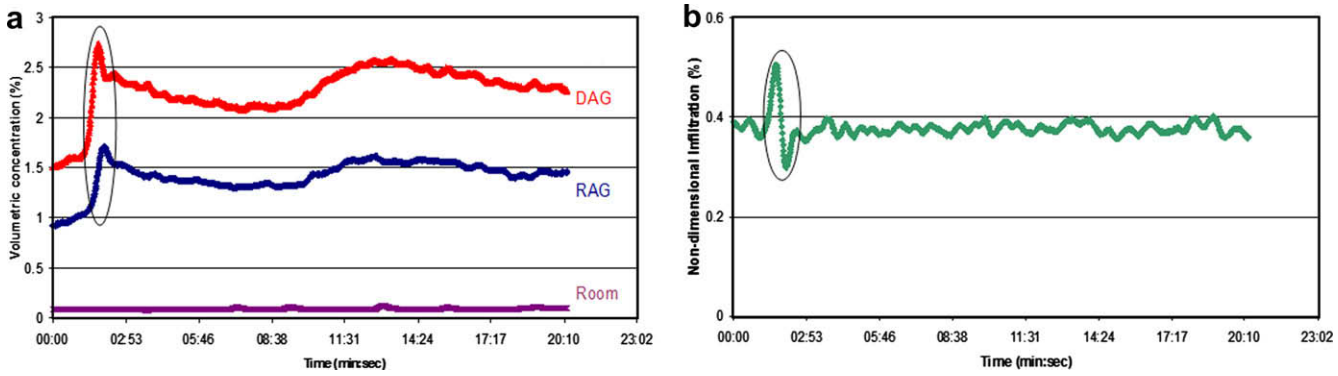

Fig. 7. (a) Volumetric concentrations and (b) non-dimensional infiltration.

place simultaneously at t_a (i.e. $\Delta t_a \to 0$), while at t_b the *NIR* is smaller than the case that $\Delta t_b \to 0$. Therefore, the existence of such delays should not be of great concerns since these small periodic changes occur during the entire test and total effect of such delays on the *NIR* may be close to zero. Our further investigation has shown that shifting the *RAG* concentration curve by about $-\Delta t_a$ or $-\Delta t_b$, before calculating the *NIR*, does not noticeably affect the *NIR* value. Such delays are functions of the speed of the flow as well as the distance between the sampling locations. It was examined when the Reynolds number (defined with the width of the *DAG* as the characteristic length) range from 2000 to 8000, this lag varies roughly between 3 and 10 s. Fig. 8 shows a delay of about 5 s for both Δt_a and Δt_b. Moreover, it is also observed that the concentrations of the *DAG* and *RAG* at higher-flow rates reach steady state much faster than lower flow rates and have less local fluctuations. Fig. 9 compares the local fluctuations at low and high flow rates. At lower flow rate, the concentrations have more fluctuations in all the regions. The fluctuations can be due to low frequency turbulence of the flow, as well as the small fluctuations that was seen in the CO_2 injection line.

For safety, the concentration of the tracer gas in the ambient should be regularly monitored to make certain that the tests are performed under the CO_2 *TLV*. CO_2 is dangerous when inhaled in high concentrations (greater than 5% by volume, equivalent to 50,000 ppm). The current *TLV* or maximum level that is considered safe for adults for an eight-hour exposure is 0.5% (5000 ppm). In Figs. 6–9 the ambient concentrations are very low and vary between 0.05% and 0.35%.

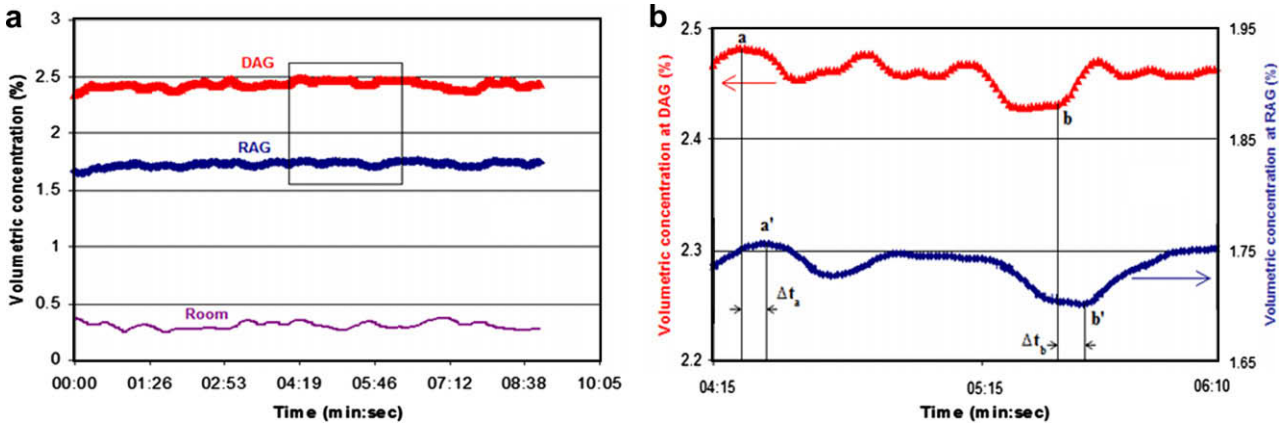

Fig. 8. Time delay between the *DAG* and *RAG*.

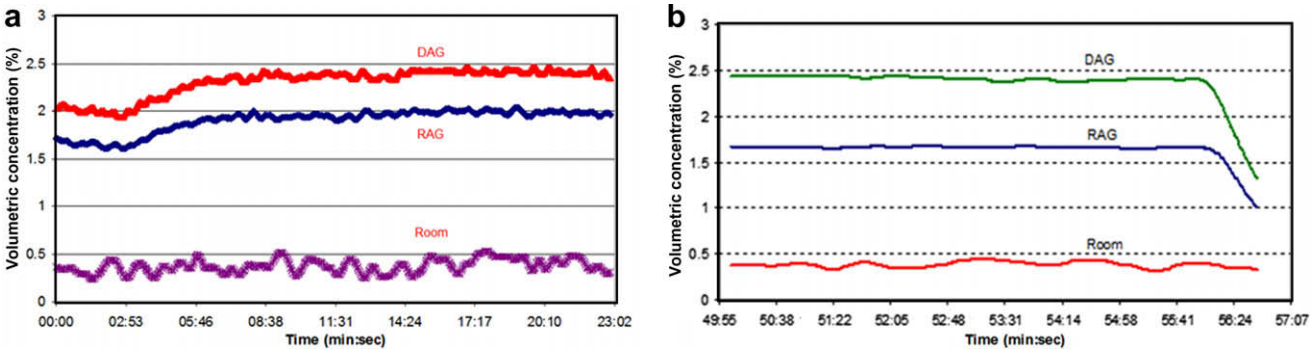

Fig. 9. Concentrations at (a) low flow rate (b) high flow rate.

To validate the tracer gas infiltration results with conventional methods, we have conducted some infiltration tests in the Refrigeration and Thermal Test Center of Southern California Edison Co. on a HillPhoenix vertical open display case that had three decks. One of the conventional methods for finding the *NIR* is based on the collected mass of condensate from the refrigeration system; by using the first law of thermodynamics this mass directly corresponds to the amount of infiltrated ambient air which brings in larger content of energy to the refrigeration system. The other method that was proposed by Rigot (1990) and Navaz et al. (2005) is based upon a temperature-dependent equation (see Eq. (15)) to calculate the infiltration rate. It should be noted, however, the correct estimation of infiltration from this equation depends on the accurate average temperature measurements at the *DAG* and the *RAG*, which in turn are contingent on precise measurements of the velocity across the width of the *DAG* and the *RAG*. This may not be easily achieved experimentally unless the measurements of temperature and velocity are performed with sufficient resolutions within the *DAG* and *RAG* widths. Nevertheless, the thermal equation is more appropriate and accurate for use in CFD simulations (Navaz et al., 2005; D'Agaro et al., 2006) as mass-weighted averaging of temperature at any location can be calculated more accurately. The verification tests were performed in an environmentally-controlled laboratory that its humidity and the temperature could be set to desired levels. The conditions of the tests were maintained at T_{Am} = 75 F (23.9 °C), $T_{DAG} \approx$ 30 F (−1.25 °C), and R.H. = 55%. Thermocouples were used to measure temperatures.

Fig. 10 compares the results of the tracer gas technique with those of the condensate-mass and thermal equation presented by Eq. (15) for two different test cases. Test case one corresponds to the test on the afore-mentioned display case configuration; while the second case is on the retrofitted display case. T_{RAG} was 44.6 F (7 °C) and 42.8 (6 °C) for Test cases one and two, respectively. The results from these different techniques are quite close.

It should be noted here that one of the advantages of this technique over others is that it can properly and precisely measure the infiltration rate during an entire refrigeration cycle: as the matter of fact, the air flow rate in an *ORDC* changes during a refrigeration cycle due to intermittent frosting and defrosting. Therefore, obtaining the knowledge about the correct instantaneous flow rate is of importance. The accurate, quick instantaneous velocity measurements across the *DAG* and *RAG*, however, may not be feasible for the temperature-dependent measurement technique (corresponding to Eq. (15)), as opposed to the current technique that can readily and precisely accomplish that even for the entire length of the cycle.

Table 1 presents the error in the flow rate at the *RAG* associated with adding CO_2 tracer gas. This error causes a small error for the absolute value of the infiltration; however, it does not affect the *NIR* within this range of added CO_2. As the results of the table indicate, the error of the mass flow rate increases linearly with increase of the concentration of the *RAG*, so does the absolute value of the infiltration rate. Thus, the excessive injection of CO_2 can increase error and is therefore not recommended. One of the problems that we encountered during the tests in this laboratory was that CO_2 partially froze after the pressure regulator and an aerosol-like flow was moving inside the injection tube. This could prevent us from achieving 25,000 ppm for the tracer gas before the *Discharge*; however, as noted previously, the absolute concentration of the injected tracer gas is not a key factor in measurement of infiltration rate.

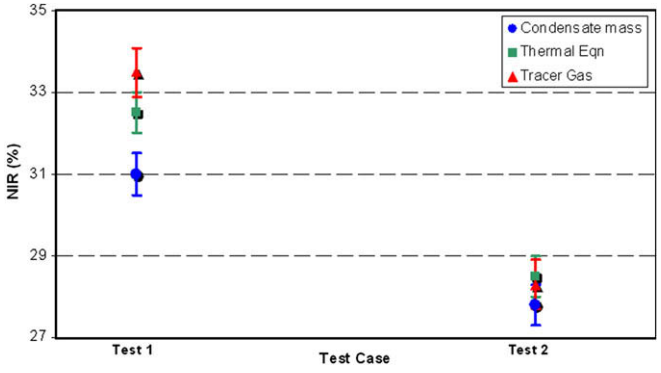

Fig. 10. Comparison of *NIR* by different methods.

7. Conclusion and recommendations

The conventional approach for measuring the amount of infiltrated ambient air into an open refrigerated display case usually takes from a few hours to a few days (for example when the condensate from the refrigeration system is collected) and may not be accurate. The new approach presented in this work, which utilizes a tracer gas technique, is fast and convenient and unlike the conventional approach is not dependent on the operation of the refrigeration system. The duration of the tests by using tracer gas can be as short as 15 min. The amount of the tracer gas that is released to the air is contingent to the type of the trace gas and also its threshold limit value (*TLV*); the concentration can be higher than *TLV* in the injected duct, but in the ambient it should be lower than the *TLV* if an operator is present in the test lab. However, the lower limit of the tracer gas concentration should be greater than the resolution of gas analyzer. It is found that the steadiness of the infiltration during the tests strongly depends on the gradients of change of concentrations, not necessarily the absolute value of the concentrations and the amount of the released tracer gas. The released tracer gas is recommended to have close molecular weight to that of the air; this will help the tracer gas to follow the path of the *primary flow* (air). It was observed that at higher speeds of air, the concentrations at all the locations tend to reach steady state faster than at lower speeds. At higher speeds, the concentrations will also experience fewer fluctuations in time and the error of the tests decreases subsequently. This new approach is suitable for both vertical and horizontal display cases.

In some circumstances where the tracer gas concentration is not constant in the ambient, three options are suggested:

1. Perform the tests in a larger facility that has proper ventilation, allowing the tests to achieve steady state.
2. Utilize a control system, which when coupled with the injection system, can adjust the concentrations of the tracer gas using the feedback from the gas analyzer. This approach can be costly.
3. Calculate the infiltration by modifying Eq. (8) and using Eq. (12), as:

$$\dot{m}_{Inf} = \frac{Q_{RAG}}{(t_2 - t_1)} \times \int_{t_1}^{t_2} \left[(C_{RAG} \times \rho_{CO_2} + (1 - C_{RAG}) \times \rho_{air}) \times \frac{C_{Dis} - C_{RAG}}{C_{Dis} - C_{Rm}} \right] dt \quad (20)$$

In the above equation, all or some of the concentrations can be functions of time. This method may require some numerical integration.

Acknowledgements

This work is sponsored in part by the US Department of Energy (under contract DE-AC05-00OR22725 with UT-Battelle, LLC.),

California Energy Commission and Southern California Edison Co. The authors would like to thank Mr. Ramin Faramarzi, the manager of Refrigeration and Thermal Test Center at Southern California Edison Co. for his long time support.

References

Axell, M., Fahlen, P. (2002). Vertical display cabinet. SP (The Swedish National Testing and Research Institute). Sweden.

ACGIH, (1971). Carbon dioxide. Documentation of the threshold limit values for substances in workroom air. In: American Conference of Governmental Industrial Hygienists, third edition, Cincinnati, OH, p. 39.

Amin, M., Navaz, H.K., Dabiri, D., Faramarzi. R., (2008). Air curtains of open refrigerated display cases revisited: a new technique for infiltration rate measurements. In: 10th International Conference on Advanced Computational Methods and Experimental Measurements in Heat Transfer, Maribor, Slovenia.

ASTM E2029-99, 2004. Standard Test Method for Volumetric and Mass Flow Measurement an a Duct Using Tracer Gas Dilution. ASTM International, West Conhshohocken, Pennsylvania.

ASHRAE Handbook of Fundamentals, (2005). American Society of Heating, Refrigeration and Air-Conditioning Engineers.

California Energy Commission (CEC) and Southern California Edison (SCE) Co., (2003). Private Communications.

Cortella, G., Manzan, M., Comini, G., 2001. CFD simulation of refrigerated display cabinets. International Journal of Refrigeration 24 (3), 250–260.

D'Agaro, P., Cortella, G., Croce, G., 2006. Two- and three-dimensional CFD applied to vertical display cabinets simulation. International Journal of Refrigeration 29, 178–190.

Faramarzi, R., Amin, M., Navaz, H.K., Dabiri, D., Rauss, M., Sarhadian, R., (2008). Air curtain stability and effectiveness in open vertical display cases. Report prepared by Southern California Edison Co. for California Energy Commission, in press.

Faramarzi, R., Sarhadian R., Coburn, B., Mitchell, S., Lutton, J., (2004). Analysis of energy enhancing measures in supermarket display cases. ASHRAE Annual Meeting, Anaheim, California.

Field, B., Kalluri, R., Loth, E., (2002). PIV investigation of air–curtain entrainment in open display cases. IIF-II-Commission D1/B1: Urbana, IL.

Field, B., Loth, E., 2006. Entrainment of refrigerated air curtains down a wall. Experimental Thermal and Fluid Science 30, 175–184.

Foster, A.M., Madge, M., Evans, J.A., 2005. The use of CFD to improve the performance of a chilled multi-deck retail display cabinet. International Journal of Refrigeration 28 (5), 698–705.

Hayes, F.C., Stoecker, W.F., 1969. Design data for air curtains. ASHRAE Transactions 2121, 153–167.

Howell, R.H., Adams, P.A., (1991). Effects of indoor space conditions on refrigerated display case performance. ASHRAE Research Project 596-RP. Department of Mechanical Engineering. University of South Florida, Tampa.

IDLH Documentation, (2007). Carbon dioxide. National Institute for Occupational Safety and Health.

Navaz, H.K., Faramarzi, R., Dabiri, D., Gharib, M., Modarress, D., 2002. The application of advanced methods in analyzing the performance of the air curtain in a refrigerated display case. ASME Journal of Fluid Engineering 124, 756–764.

Navaz, H.K., Henderson, B.S., Faramarzi, R., Pourmovahed, A., Taugwalder, F., 2005. Jet entrainment rate in air curtain of open refrigerated display cases. International Journal of Refrigeration 28 (2), 267–275.

Rigot, G., (1990). Meubles et vitrines frigorifiques, Pyc ed, Paris, France.

Rouaud, O., Havet, M., 2006. Behavior of an air curtain subjected to transversal pressure variations. Journal of Environmental Engineering 132 (2), 263–270.

Stribling, D., Tassou, S.A., Mariott, D., 1997. A two-dimensional CFD model of a refrigerated display case. ASHRAE Transactions 104, 88–94.

The Fluent© code. (2007), Fluent Inc.